Paleobiology

Early and Middle Triassic trends in diversity, evenness, and size of foraminifers on a carbonate platform in south China: implications for tempo and mode of biotic recovery from the end-Permian mass extinction

Jonathan L. Payne, Mindi Summers, Brianna L. Rego, Demir Altiner, Jiayong Wei, Meiyi Yu, and Daniel J. Lehrmann

Early and Middle Triassic trends in diversity, evenness, and size of foraminifers on a carbonate platform in south China: implications for tempo and mode of biotic recovery from the end-Permian mass extinction

Jonathan L. Payne, Mindi Summers, Brianna L. Rego, Demir Altiner, Jiayong Wei, Meiyi Yu, and Daniel J. Lehrmann

Abstract.—Delayed biotic recovery from the end-Permian mass extinction has long been interpreted to result from environmental inhibition. Recently, evidence of more rapid recovery has begun to emerge, suggesting the role of environmental inhibition was previously overestimated. However, there have been few high-resolution taxonomic and ecological studies spanning the full Early and Middle Triassic recovery interval, leaving the precise pattern of recovery and underlying mechanisms poorly constrained. In this study, we document Early and Middle Triassic trends in taxonomic diversity, assemblage evenness, and size distribution of benthic foraminifers on an exceptionally exposed carbonate platform in south China. We observe gradual increases in all metrics through Early Triassic and earliest Middle Triassic time, with stable values reached early in the Anisian. There is little support in our data set for a substantial Early Triassic lag interval during the recovery of foraminifers or for a stepwise recovery pattern. The recovery pattern of foraminifers on the GBG corresponds well with available global data for this taxon and appears to parallel that of many benthic invertebrate clades. Early Triassic diversity increase in foraminifers was more gradual than in ammonoids and conodonts. However, foraminifers continued to increase in diversity, size, and evenness into Middle Triassic time, whereas diversity of ammonoids and conodonts declined. These contrasts suggest decoupling of recovery between benthic and pelagic environments; it is unclear whether these discrepancies reflect inherent contrasts in their evolutionary dynamics or the differential impact of Early Triassic ocean anoxia or associated environmental parameters on benthic ecosystems.

Jonathan L. Payne, Mindi Summers,* and Brianna L. Rego. Department of Geological and Environmental Sciences, Stanford University, Stanford, California 94305. E-mail: jlpayne@stanford.edu. *Present address: Scripps Institution of Oceanography, University of California at San Diego, 9500 Gilman Drive, La Jolla, California 92093

Demir Altiner. Department of Geological Engineering, Middle East Technical University, Ankara 06531, Turkey

Jiayong Wei. Guizhou Geological Survey, Bagongli, Guiyang 550011, Guizhou Province, China

Meiyi Yu. College of Resource and Environment Engineering, Guizhou University, Caijiaguan, Guiyang 550003, Guizhou Province, China

Daniel J. Lehrmann. Department of Geology, University of Wisconsin-Oshkosh, 800 Algoma Boulevard, Oshkosh, Wisconsin 54901. Present address: *Department of Geosciences, Trinity University, One Trinity Place, San Antonio, Texas 78212*

Introduction

Recovery from the end-Permian mass extinction has long been viewed as more protracted than that following other mass extinctions (Hallam 1991; Erwin 1993, 2001). Lower Triassic marine communities typically exhibit low taxonomic diversity, low evenness (i.e., dominance of communities by a few very abundant species), and the absence of large species (Schubert and Bottjer 1995; Twitchett and Wignall 1996; Twitchett 1999; Rodland and Bottjer 2001; Fraiser and Bottjer 2004, 2005; Payne 2005; Payne et al. 2006a). The rarity or absence of biogenic sedimentary deposits such as reefs, coal, and chert from Lower Triassic strata (Flügel 1994; Retallack et al. 1996; Beauchamp and Baud 2002; Flügel 2002; Pruss and Bottjer 2004) and limited contribution of skeletal grains to carbonate sediments (Payne et al. 2006a) suggest a greatly reduced role for skeletal animals and algae in biogeochemical cycles. For most marine clades and ecosystems, increases in taxonomic diversity and ecological complexity appear to be largely Middle Triassic

phenomena (Hallam 1991; Erwin 1993, 2001). This Early Triassic lag interval has been widely interpreted to result from environmental inhibition of biotic recovery. Ocean anoxia, low primary productivity, extreme climate warmth, and episodic environmental disturbance driven by Siberian Traps volcanic eruptions have all been proposed as inhibitors of recovery (e.g., Hallam 1991; Retallack 1999; Twitchett 1999, 2001, 2007; Payne et al. 2004; Twitchett et al. 2004; Payne et al. 2006a; Fraiser and Bottjer 2007; Knoll et al. 2007).

Recently, evidence for more rapid Early Triassic diversification has emerged, raising questions about the extent to which recovery from the end-Permian mass extinction was in fact inhibited by ongoing environmental disturbance. Brayard et al. (2009) observed rapid taxonomic diversification of ammonoids within the first 2 Myr of Early Triassic time, leading them to question the extent of environmental inhibition of recovery at the global scale. They proposed that the apparent delay in recovery for many other marine taxa may be exaggerated by the poor quality or limited sampling of the Lower Triassic fossil record. Conodonts also exhibit a pattern of rapid diversification during Early Triassic time (Orchard 2007; Stanley 2009). A handful of more diverse and complex benthic body fossil and ichnofossil assemblages have been reported from lowermost Triassic strata in recent years (Twitchett et al. 2004; Beatty et al. 2008). Similarly, a recent report of Early Triassic gastropods larger than those previously described suggested more limited size reduction or more rapid size increase than previously suspected (Brayard et al. 2010).

At present, most evidence for more rapid recovery in the marine realm derives from pelagic taxa, whereas most evidence for delayed recovery derives from benthic taxa. Thus, the differences in timing of recovery could be genuine, resulting from contrasting controls on recovery in benthic and pelagic ecosystems. Alternatively, apparent differences in the tempo of recovery may result largely from differences in sampling of benthic versus pelagic taxa (Brayard et al. 2009, 2010) or in the local environments sampled (Beatty et al. 2008). A sampling control is
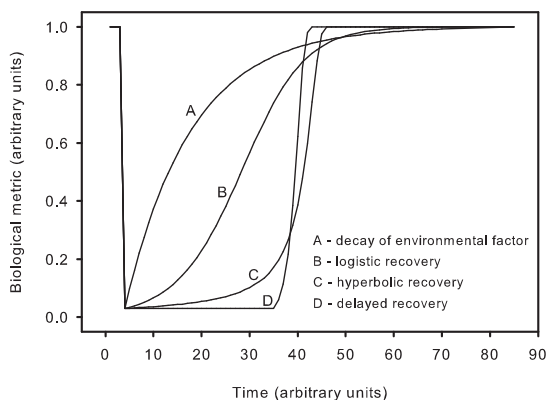

FIGURE 1. Expected trajectories under the exponential decay of an environmental control (A), a slow logistic recovery with no delay (B), a hyperbolic recovery with no delay (C), and a delay followed by rapid logistic recovery (D). All scenarios give similar times to full recovery. Given a known time to full recovery, and ignoring issues of sampling, controls on recovery can be identified from the observed trajectory. In practice, distinguishing unambiguously among possibilities may be challenging. In the example presented here, delayed recovery followed by a rapid logistic trajectory bears close similarity to a hyperbolic trajectory with no delay.

supported by the fact that the pelagic organisms known to diversify quickly are also those taxa used most often in Lower Triassic biostratigraphy and so may be expected to have been sampled and studied more intensively than most benthic fossils. Distinguishing between these possibilities requires high-resolution taxonomic and ecological data on the recovery of benthic organisms.

Ideally, discrimination among hypothesized recovery modes is achieved by comparison to mathematical representations. In the simplest case, delayed recovery is distinguished from immediate recovery by an interval with no identifiable increase in diversity (or another chosen metric), whereas immediate recovery exhibits no distinct ''lag'' interval (Fig. 1). In reality, the situation is more challenging because the expected trajectory of recovery depends upon assumptions about how diversity (or another metric) is controlled. For example, diversity-dependent origination and extinction dynamics with a fixed carrying capacity produce a logistic curve (Fig. 1). If ecological processes influence carrying capacity, however, then the trajectory will deviate from a logistic curve. For example, positive feedback from

ecological interactions may produce a hyperbolic recovery trajectory (Erwin 2007), illustrated in Figure 1. Nearly all biologically controlled models for recovery predict an initially concave recovery trajectory (Erwin 2007; Brayard et al. 2009), which might be mistaken for an environmentally controlled lag interval (Fig. 1).

Recovery trajectories may also vary among ecological groups. For example, Solé et al. (2002) modeled recovery of populations and diversity in communities following disturbance and found that although primary producers in a community began to recover immediately, primary and secondary consumers experienced substantial lag intervals.

Finally, environmental control can produce recovery trajectories other than a simple lag interval prior to diversification. For example, if a hypothetical extinction were caused by rapid CO_2 emission to the atmosphere and oceans and recovery were controlled by pCO_2 (e.g., via temperature), one would expect a convex recovery trajectory reflecting the roughly exponential decline in pCO_2 as it was consumed by various geochemical feedback mechanisms (Fig. 1). More complex environmental dynamics could, in principle, result in more complex recovery trajectories. Such a possibility is hinted at for the Early Triassic by the occurrence of several large carbon isotope excursions (Payne et al. 2004) and episodes of shallow-marine anoxia (Wignall and Twitchett 2002).

Because the recovery trajectories associated with various processes may be difficult to distinguish by using diversity data alone, particularly when temporal resolution is limited, use of multiple recovery metrics in parallel may provide additional discriminating power. For example, low oxygen availability might not impede diversification but could be reflected in the size structure of the biota. Alternatively, taxonomic diversity and size could recover rapidly while community evenness remains low during a period of ecological restructuring. In principle, decoupling of recovery trajectories among several metrics could provide a paleobiological fingerprint of recovery dynamics and controls.

In this study, we present a record of taxonomic and ecological recovery in benthic foraminifers through the Early and Middle Triassic from an exceptionally exposed, isolated carbonate platform in southern China. Sampling of stratigraphic sections representing both shallow-water platform interior and deep-water basin margin depositional settings allows us to distinguish the effects of spatial gradients in diversity and ecosystem structure from platform-wide patterns of biotic recovery. These data improve our ability to compare recovery dynamics between benthic and pelagic taxa, as well as the extent of coupling between taxonomic and ecological aspects of recovery.

Geological Setting

The Great Bank of Guizhou (GBG) is an Upper Permian to Upper Triassic isolated carbonate platform. It sits within the Nanpanjiang Basin, a deep marine embayment into the Yangtze Block of southern China (Fig. 2A), located in the eastern equatorial Tethys during Triassic time (Lehrmann et al. 1998). The GBG developed on a remnant topographic high following Late Permian step-back of the Yangtze Platform margin, evolving from a low-relief carbonate bank in Early Triassic time to a high-relief platform bordered by erosional escarpments before the end of the Middle Triassic (Lehrmann et al. 1998). Upper Permian through Middle Triassic strata of the GBG are exposed on the east limb of a faulted syncline in both shallow-water platform interior and deep-water basin margin environments (Fig. 2B). Lower and Middle Triassic strata are together more than 1.5 km thick in the platform interior and more than 600 m thick on the basin margin (Lehrmann et al. 1998).

Previous studies of the GBG have addressed platform architecture (Lehrmann et al. 1998), tectonic controls on platform drowning (Lehrmann et al. 1998; Lehrmann et al. 2007), Permian/Triassic boundary and Early Triassic lithofacies (Lehrmann 1999; Lehrmann et al. 2001, 2003; Yang and Lehrmann 2003; Adachi et al. 2004; Payne et al. 2006a, 2007; Ezaki et al. 2008), the Anisian platform-margin *Tubiphytes* reef (Payne et al. 2006b),
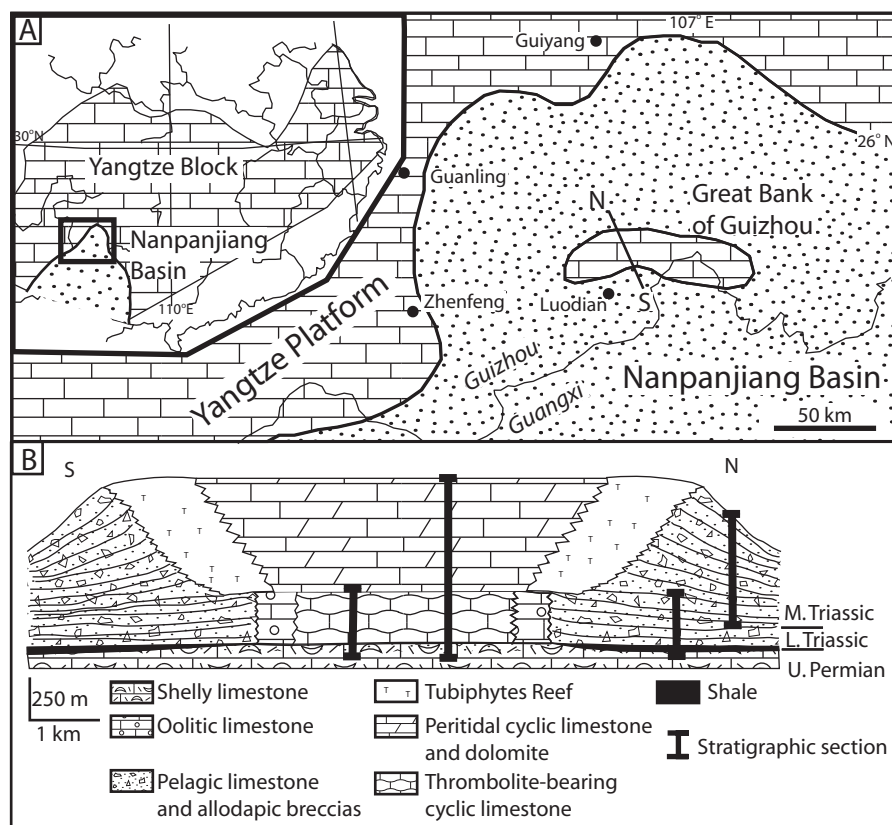
FIGURE 2. Geological setting. A, Schematic geological map of the Nanpanjiang Basin. B, Schematic cross-section of the GBG, illustrating the positions of sampled sections. Modified from Lehrmann et al. (2006).

and the carbon isotope stratigraphy of the Permian/Triassic boundary (Krull et al. 2004) and Early Middle Triassic recovery interval (Payne et al. 2004; Tong et al. 2007). Payne et al. (2006a) used measured thicknesses of lithofacies in stratigraphic sections and point counts of thin sections to quantify the proportional contributions of skeletal and non-skeletal carbonate phases to Late Permian through Middle Triassic strata on the GBG. They found that the skeletal content of platform strata decreased dramatically across the Permian/Triassic boundary in both shallow- and deep-water environments. Subsequent increase in skeletal abundance did not begin until late in the Early Triassic. Foraminifera form more than 2% of the rock by volume in Upper Permian strata on the GBG, then persist as trace components (<0.1%) through most of the Lower Triassic before increasing to 0.1% to 0.2% of the rock volume in Spathian, Anisian, and Ladinian strata.

Foraminiferan tests constitute a smaller fraction of shell debris than mollusks, echinoderms, and the microproblematicum *Tubiphytes*—only a few percent of the total skeletal material in most stages (Payne et al. 2006a). The GBG is qualitatively similar to many other carbonate platforms and ramps in terms of the presence and relative abundance of lithofacies (Lehrmann et al. 2001; Pruss et al. 2005a,b, 2006; Payne et al. 2006a; Baud et al. 2007), although the precise extent of quantitative similarity has yet to be determined (Jacobsen et al. 2010).

Methods

We examined a suite of 598 thin sections collected from two basin margin and two platform interior stratigraphic sections to assess the Early Middle Triassic recovery of foraminifers on the GBG (Fig. 2). A composite timescale for the samples was developed using conodont biostratigraphy and lithostra-

tigraphy, supplemented by magnetostratigraphy and carbon isotope stratigraphy (Lehrmann et al. 1998, 2006; Payne et al. 2004). Recent radiometric age constraints for the Triassic timescale from Lehrmann et al. (2006), Mundil et al. (1996, 2004), Ovtcharova et al. (2006), and Galfetti et al. (2007a) were used to develop an age model for the strata, assuming uniform sedimentation rates between radiometric calibration points and equal durations of all substages when multiple substages occurred between consecutive radiometric tie-points. The Aegean and Bithynian substages of the Anisian (Middle Triassic) were binned together because the boundary between them could not be determined with sufficient precision.

From the 598 thin sections examined, 499 contained at least one skeletal grain (of any sort) and 239 contained at least one foraminifer. For each foraminiferan-bearing sample, we counted the number of identifiable specimens belonging to each genus (and species where possible). In total, 1631 specimens were assignable at least to genus level. We photographed 1052 of the identifiable specimens, including at least one specimen per genus (or species) from each sample, focusing on the largest and best-preserved specimens from each taxon, yielding 498 size maxima for genera within samples. Maximum linear dimension is highly correlated with biovolume, capturing approximately 90% of variance in biovolume in a study of diverse fossil groups, and therefore can serve as a meaningful size metric (Novack-Gottshall 2008). Rarefaction and evenness (Hurlbert's [1971] PIE [probability of interspecific encounter]) calculations were performed for each substage with PAST (Hammer et al. 2001) using pooled abundances among samples within each substage.

Occurrence and size data are archived at Data Dryad (www.datadryad.org) and can be accessed at http://dx.doi.org/10.5061/dryad.7855.

Results

Diversity and Evenness.—Figure 3 illustrates the local occurrence patterns and stratigraphic ranges of foraminifers by genus. Raw genus diversity increased from five genera in the Griesbachian substage (earliest Triassic) to a maximum of 34 genera in the Pelsonian (middle Anisian). Substantial taxonomic turnover occurred during the Griesbachian through Smithian substages; only four of the 11 genera present during this interval persist into younger strata (Fig. 3). In contrast, all genera observed in Spathian samples persist into the Anisian, where they co-occur with numerous new genera.

The broad trend of increase in raw genus diversity appears to result from true increases in local evenness and taxonomic richness. In fact, sampling-standardized diversity and evenness increase between the Griesbachian and Dienerian substages, whereas raw genus diversity decreased from five genera to four. Rarefaction curves relating the number of individuals sampled to the expected genus diversity increase in slope steadily from the Griesbachian through Aegean/Bithynian before stabilizing in the Middle Triassic; this pattern is apparent across the platform as a whole (Fig. 4A) and within depositional environments (Fig. 4B,C). Rarefied genus diversity on the GBG increases nearly linearly from the Griesbachian through Pelsonian at standardized sample sizes of 44 and 100 individuals (Fig. 4D). Evenness increases monotonically through the Early Triassic from a Griesbachian low of 0.08, stabilizing near 0.90 at the beginning of the Anisian (Fig. 4E). After accounting for variation in sampling among stages, there is indication of neither a multi-substage lag interval preceding increase in diversity and evenness nor accelerating recovery through Early Triassic.

Comparison between platform-interior and basin-margin environments demonstrates a clear spatial gradient in diversity across the platform (Figs. 4, 5). During the Griesbachian and Dienerian, foraminifers occur only in platform interior sections. Within-sample diversity values are similar between the platform interior and basin margin during the Smithian. In contrast, basin margin samples exhibit much greater diversity during the Middle Triassic than do coeval platform interior samples. However, the number of co-occurring taxa increased through time within both platform-interior
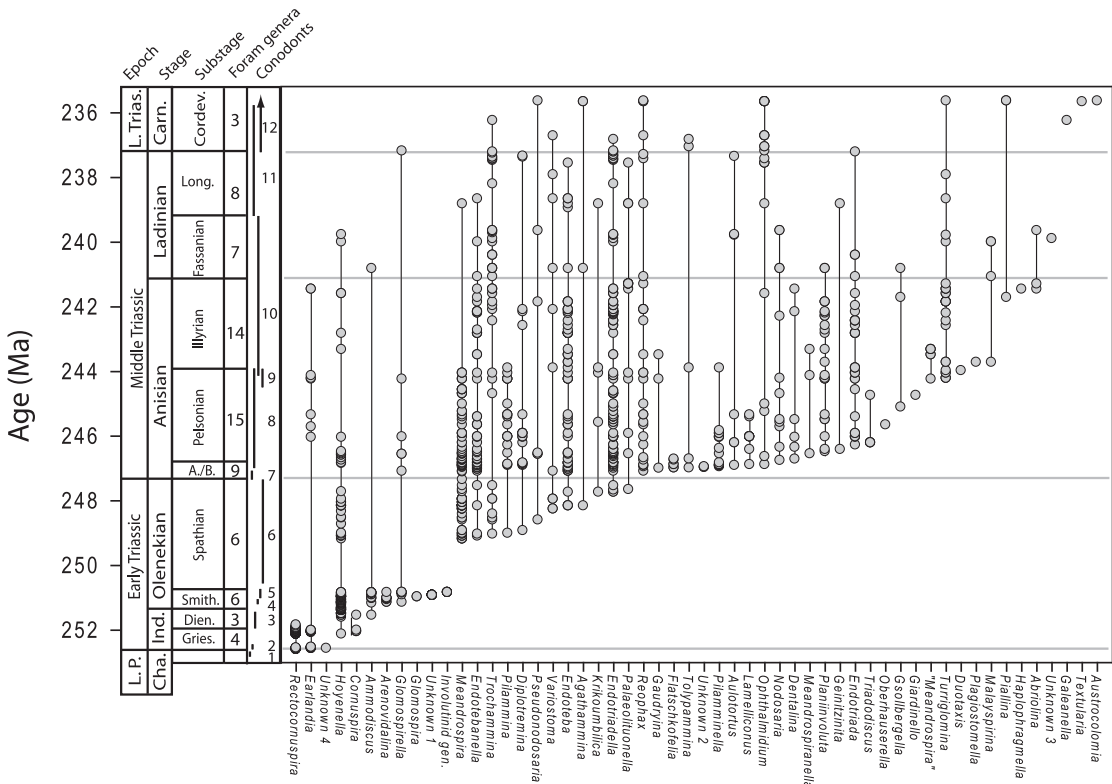
FIGURE 3. Occurrences of foraminifers by genus. Biostratigraphic age constraints based upon conodont occurrences, as reported in Payne et al. (2004). Absolute age constraints based upon data in Mundil et al. (1996, 2004), Lehrmann et al. (2006), Ovtcharova et al. (2006), and Galfetti et al. (2007a). L.P., Late Permian; Cha., Changhsingian; Ind., Induan; Gries., Griesbachian; Dien., Dienerian; Smith., Smithian; A./B., Aegean–Bithynian; Long., Longobardian; Cordev., Cordevolian; Carn., Carnian; L. Trias., Late Triassic. Conodonts: 1, *Neogondolella changxingensis*; 2, *Hindeodus parvus*; 3, *Neospathodus dieneri*; 4, *Ns. waageni*; 5, *Ns. bransoni*; 6, *Ns. homeri/symmetricus*; 7, *Chiosella timorensis*; 8, *Nicoraella germanicus/kockeli*; 9, *Paragondolella bulgarica*; 10, *Ng. constricta*; 11, *Budurovignathus mungoensis*; 12, *Metapolygnathus polygnathiformis*.

and basin-margin settings (Fig. 5). No Griesbachian, Dienerian, or Smithian sample contains more than three genera, whereas the mode for within-sample diversity was four genera during the Pelsonian; all Middle Triassic substages contain at least one sample with seven or more genera (Fig. 5). One Pelsonian sample (representing just a few square centimeters or rock) contains 14 genera, more than occur in any Early Triassic substage (Fig. 5). Most diversity changes between successive stages from the Griesbachian through Aegean-Bithynian are statistically significant, whereas those during the Middle Triassic are not (Table 1). This pattern holds both for the platform as a whole and within depositional environments (Table 1). However, differences in diversity between

environments are significant during Middle Triassic time (Table 1). Thus, local taxonomic diversification can be observed within stratigraphic sections, but the apparent extent of diversification is muted when considering the platform interior alone and exaggerated when considering only the basin margin.

Local taxonomic diversification of foraminifers on the GBG follows a trajectory broadly similar to that observed in other regions and in global compilations. Genus diversity for the Induan (Griesbachian and Dienerian) on the GBG is more than half of the global value reported for this interval by Groves and Altiner (2005). The taxonomic composition of Griesbachian foraminifers on the GBG is similar to that reported at other Tethyan localities (Groves et al. 2005, 2007; Song et
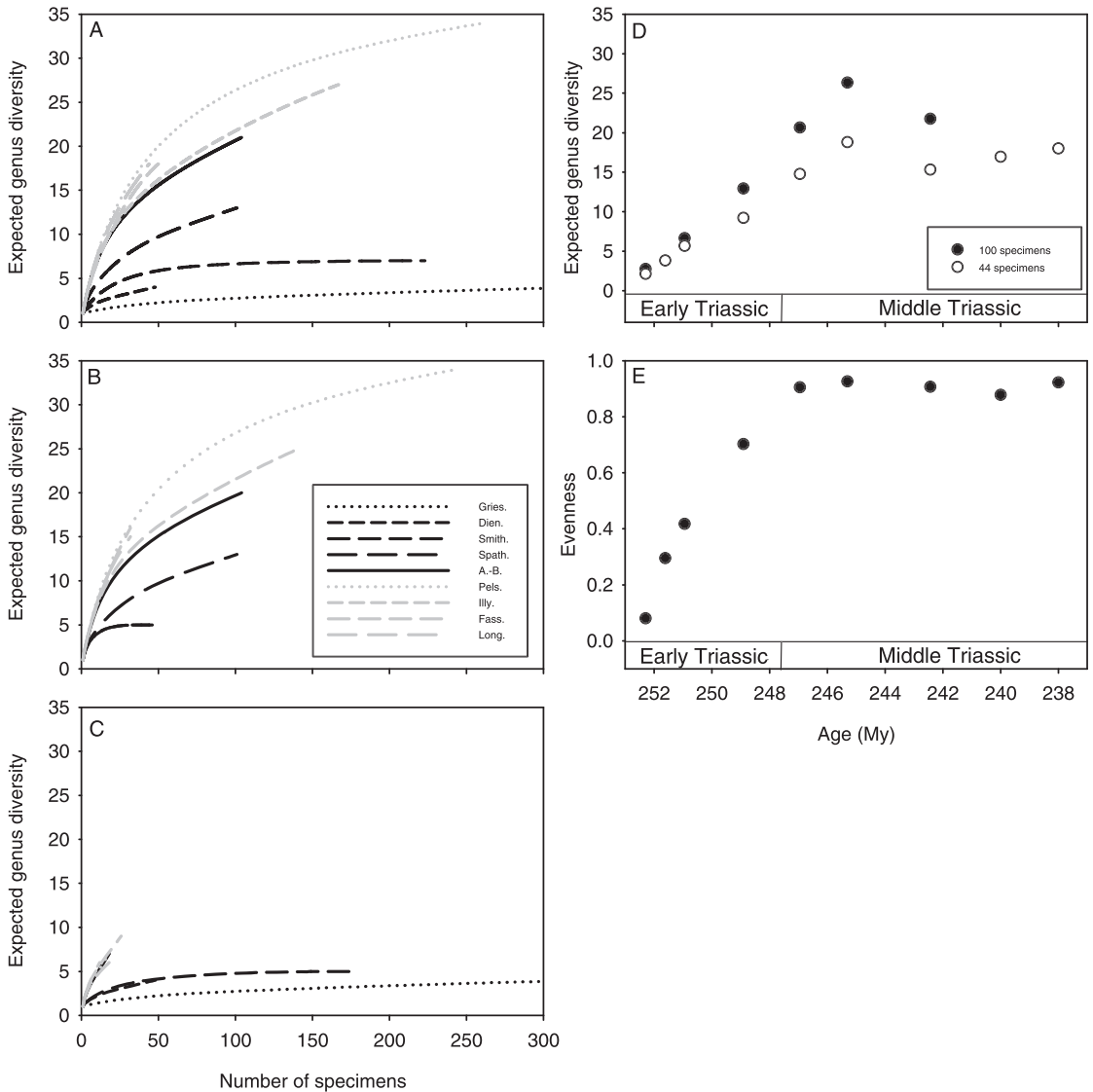
FIGURE 4. Metrics of foraminiferan diversity through the Early and Middle Triassic, illustrating the gradual increase in diversity through the Early Triassic and stabilization early in the Middle Triassic. Increasing diversity is also associated with increasing evenness, a measure of how equitably individuals are distributed among species or genera with zero being the minimum and one being the maximum possible value. A–C, Rarefaction curves for Early and Middle Triassic substages illustrating expected genus diversity versus number of individuals sampled for the entire platform (A), for the basin margin environment (B), and for the platform interior environment (C). D, Substage trends in expected genus diversity at sample sizes of 44 and 100 specimens. E, Substage trend in evenness through the Early and Middle Triassic. Abbreviations: Spath, Spathian; Pels., Pelsonian; Illy., Illyrian; Fass., Fassanian. All other abbreviations as in Figure 3.

al. 2007), as is the numerical dominance of *Earlandia* spp. and *Rectocornuspira kalhori* within Griesbachian strata (Fig. 6) (Groves and Altiner 2005). Genus diversity on the GBG during the Olenekian (Smithian and Spathian) is greater than the global value reported by Groves and Altiner (2005) for three reasons. First, Groves and Altiner did

not include textulariids in their analysis, which addressed only calcareous clades. Therefore, genera such as *Trochammina* and *Pilammina* were excluded from their analysis. Second, we have included taxa in open nomenclature from the Smithian of the GBG in our diversity count because they are clearly distinct from the other genera present. For
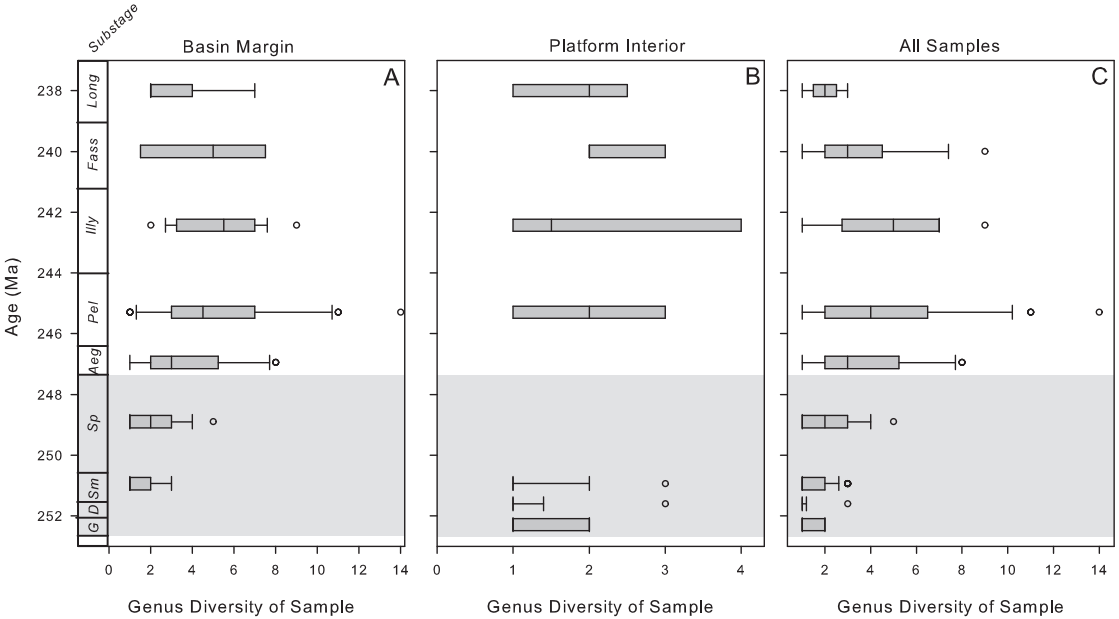
FIGURE 5. Boxplots illustrating the distribution of genus diversity within individual thin sections by substage, showing trends of increasing within-sample diversity from the Lower to Middle Triassic. A, Basin margin samples. B, Platform interior samples. C, All samples. Abbreviations: G, Griesbachian; D, Dienerian; Sm, Smithian; Sp, Spathian; Aeg, Aegean–Bithynian; Pel, Pelsonian; Illy, Illyrian; Fass, Fassanian; Long, Longobardian.

example, the involutinid genus we report is one of the earliest records for the order Involutinida in the Tethyan Triassic. Third, some taxa (e.g., *Endotebanella* and the duostominid genera) occur within the uppermost Spathian on the GBG but were previously known only from Anisian and younger strata (Groves and Altiner 2005). More detailed quantitative comparison of diversity increase on the GBG and at other localities is currently impossible because of the paucity of published abundance data, particularly for the

Olenekian and Middle Triassic. The lack of local abundance data in the literature also prevents any direct comparison between Late Permian and Early Triassic communities; however, co-occurrences of numerous genera within latest Permian samples on the GBG (Song et al. 2009) and elsewhere (Groves et al. 2005, 2007; Song et al. 2007) suggest that evenness was quite high prior to the mass extinction event.

Size.—Trends in test size provide a diversity-independent metric of biotic recovery.

TABLE 1. Results from tests of significance for differences in sample-level diversity between substages and environments. All values are *p*-values from Mann-Whitney tests. For all categories other than environment, the *p*-value represents a comparison of the stated stage to the succeeding stage. For Environment, the comparison was between platform interior and basin margin samples from the same stage. Boldface values indicate statistically significant differences at α = 0.05.

Stage	GBG sample diversity	Interior diversity	Basin diversity	Environment
Griesbachian	**0.04**	**0.04**		
Dienerian	0.09	0.09		
Smithian	**0.0002**	0.11 (vs. Pelsonian)	**0.0002**	0.11
Spathian	0.06		0.06	
Aegean–Bithynian	0.18		0.06	
Pelsonian	0.81	**0.03**	0.73	**0.02**
Illyrian	0.10	**0.03**	0.90	**0.02**
Fassanian	0.59	0.90	0.27	0.28
Longobardian				0.09
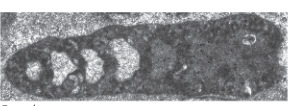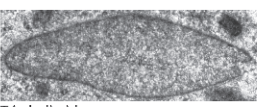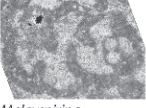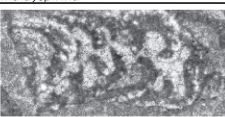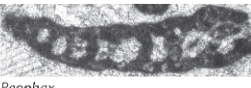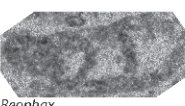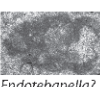
Epoch	Stage	Substage	Largest specimen	Most abundant genus
Late Triassic	Carnian	Cordevolian	Reophax	28.6% Ophthalmidium
Middle Triassic	Ladinian	Longobardian	Triadodiscidae	15.9% Endotriadella
Middle Triassic	Ladinian	Fassanian	Malayspirina	30.0% Trochammina
Middle Triassic	Anisian	Illyrian	Malayspirina?	19.2% Endotriadella
Middle Triassic	Anisian	Pelsonian	Reophax	18.0% Endotriadella
Middle Triassic	Anisian	Aegean/Bithynian	Reophax	19.2% Meandrospira
Early Triassic	Olenekian	Spathian	Endotebanella?	49.5% Meandrospira
Early Triassic	Olenekian	Smithian	Unknown genus	75.2% Hoyenella
Early Triassic	Induan	Dienerian	Ammodiscus?	83.3% Hoyenella
Early Triassic	Induan	Griesbachian	Earlandia	95.9% Rectocornuspira

FIGURE 6. Illustrations of the largest and most abundant foraminifera by substage. The percentage of specimens represented by the most common genus is also reported.

The sizes of the largest specimens and the most common genera on the GBG decreased from the Griesbachian to Dienerian; they then increased steadily through the remainder of the Early Triassic before stabilizing early in the Anisian (Table 2; Figs. 6–8). Comparison to genus-level size data for the Late Permian on the GBG, compiled from figures published by Song et al. (2009), reveal dramatic decrease in maximum and mean size across the end-Permian extinction event (Fig. 7D). Middle Triassic size distributions are similar to their latest Permian counterparts (Fig. 7D). Early Triassic increase in median and maximum size among genera is apparent in both platform interior and basin margin environments, as well as across the platform as a whole, indicating that differential sampling of environments harboring smaller and larger taxa does not account for the observed trend. The size distribution of specimens changes significantly across a substantial fraction of substage transitions from the Griesbachian through Aegean-Bithynian but is absent during the Middle Triassic (Table 2). This pattern holds both for the platform as a whole and within depositional environments (Table 2). Analysis using only genus maxima does not reveal significant size change across substage transitions (Table 2), but low diversity during the Early Triassic limits statistical power. Unlike the results for diversity, there is no indication of a spatial gradient in the size distribution (Table 2). Size increase occurred across all measured specimens and across all taxa (using genus size maxima) (Fig. 7).

To further test the influence of local environmental factors on observed size trends, we compiled a size database of Late Permian through Middle Triassic foraminifers from published monographs (Schell and Clark 1960; Schroeder 1968; Zaninetti 1976; Salaj et al. 1983; Rettori 1995; Leven and Okay 1996; Kobayashi 1997; Hauser et al. 2001; Pronina-Nestell and Nestell 2001; Apthorpe 2003; Unal et al. 2003; Kobayashi 2004, 2005; Kobayashi et al. 2005; Groves et al. 2007; Song et al. 2007, 2009; Vuks 2007), measuring the maximum linear dimension of all figured specimens. Taxonomic assignments were standardized following Rettori (1995). Trends

TABLE 2. Results from tests of significance for size differences between substages and environments. We compared sizes using all measured specimens, only size maxima for genera, and all specimens by environment. All values are *p*-values from Mann-Whitney tests. For all categories other than environment, the *p*-value represents a comparison of the stated stage to the succeeding stage. For environment, the comparison was between platform interior and basin margin specimens from the same stage. Boldface values indicate statistically significant differences at α = 0.05.

Stage	GBG specimens	GBG genera	Interior specimens	Basin specimens	Environment
Griesbachian	**0.03**	0.14	**0.03**		
Dienerian	0.10	0.06	0.10		
Smithian	**0.006**	0.55	0.04 (vs. Pelsonian)	**0.006**	0.60
Spathian	**0.008**	0.07		**0.008**	
Aegean–Bithynian	0.25	0.23		0.28	
Pelsonian	0.69	0.24	0.28	0.65	0.66
Illyrian	0.28	0.83	0.94	0.22	0.40
Fassanian	0.10	0.40	0.85	0.06	0.63
Longobardian					0.88

in the literature data are largely concordant with those on the GBG (Fig. 7D,E); both exhibit dramatic reduction in mean and maximum size from the Changhsingian to the Induan and a gradual increase in these values from the Induan through Anisian. Importantly, none of the Early Triassic species in the literature data set are as large as the largest Aegean-Bithynian specimens from the GBG, demonstrating that the rapid size increase on the GBG does not merely reflect the local immigration of larger species that were common elsewhere during the Early Triassic. Although the more limited temporal resolution of the literature data does not permit assessment of a global size decrease

between the Griesbachian and Dienerian nor detailed comparison of the timing of stabilization in the size distribution, there is no evidence of substantial discordance between evolutionary trends observed on the GBG and those occurring over much broader spatial scales.

Size increase on the GBG from the Griesbachian through Aegean-Bithynian occurred both through the preferential origination of larger taxa and through a tendency toward size increase within species and genera. There is a significant correlation between the size of the oldest recorded specimen in a genus and the age of its first occurrence for those taxa that first occur during the Griesbachian
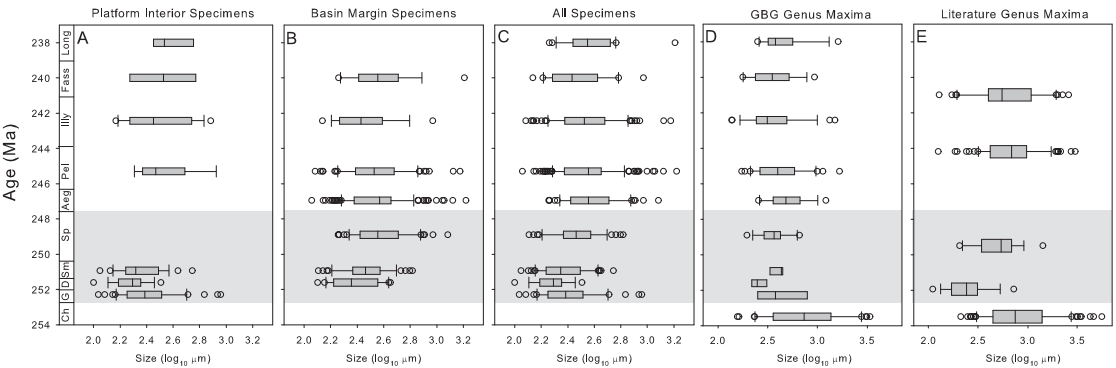
FIGURE 7. Boxplots of foraminifer sizes through the Early Triassic, illustrating size decrease across the Permian/Triassic boundary, size increase from the Early Triassic into the early part of the Middle Triassic, and Middle Triassic stabilization. A, Distribution of sizes for all measured specimens from the GBG platform interior. B, Distribution of sizes for all measured specimens from the GBG basin margin. C, Distribution of sizes for all measured specimens on the GBG. D, Distribution of genus maximum sizes for the GBG. Changhsingian specimens measured from Song et al. (2009). E, Distribution of genus maximum sizes from our literature database, not including specimens measured as part of this study. Stratigraphic resolution is coarser in the literature data: Griesbachian box represents Induan data (Griesbachian and Dienerian); Smithian box represents Olenekian data (Smithian and Spathian); Aegean–Bithynian box represents all Anisian data; Fassanian box represents all Ladinian data. Boxes encompass 25th through 75th percentiles, with the median marked by a central line. Whiskers denote 10th and 90th percentiles. Points denote observations below the 10th or above the 90th percentile. Abbreviations: Ch, Changhsingian; all others as in Figure 5.
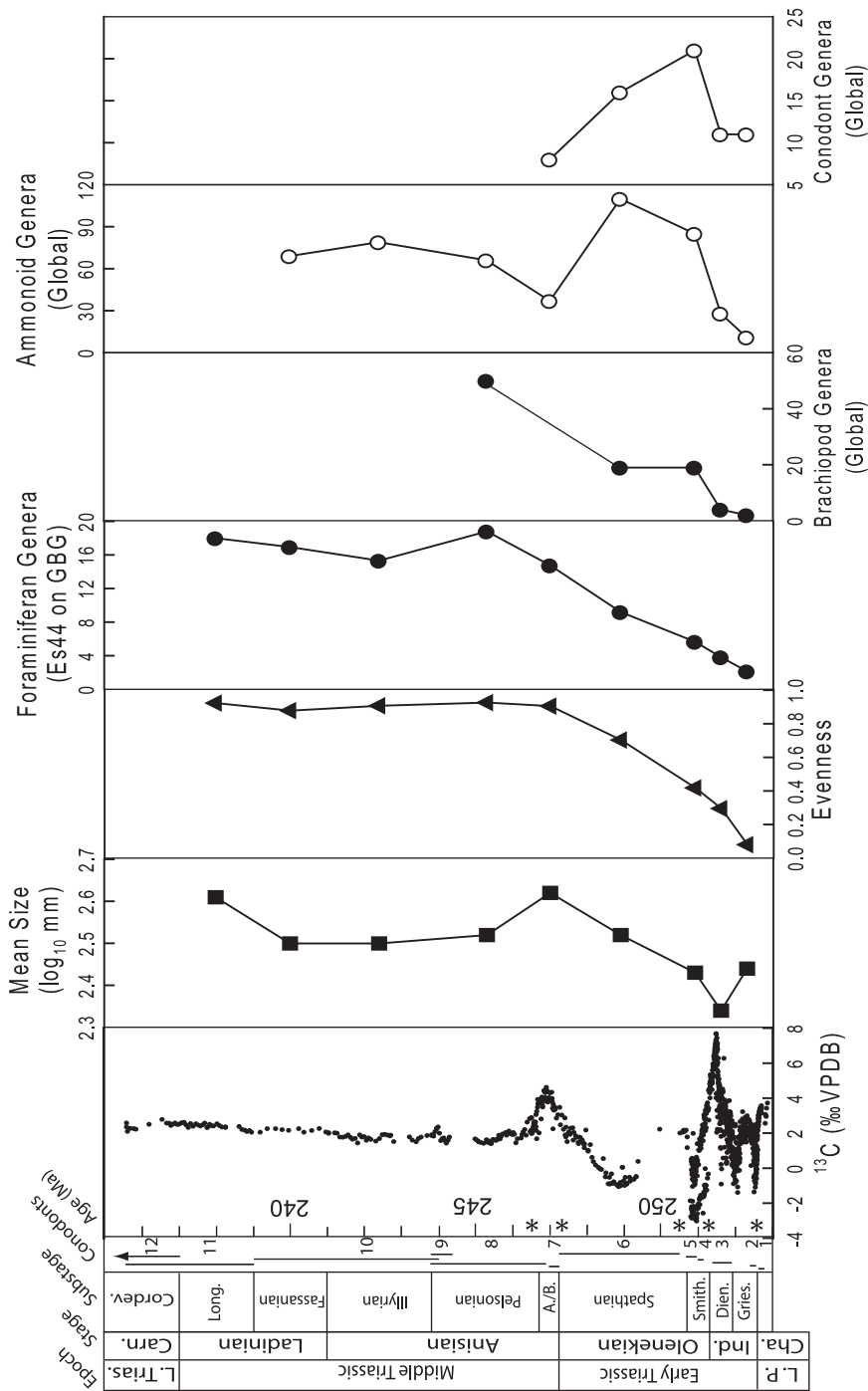
FIGURE 8. Comparison of foraminiferan recovery metrics to $\delta^{13}C$ variation and the diversity histories of brachiopods, ammonoids, and conodonts. Foraminifers exhibit a gradual recovery through Early Triassic time, with ecological and taxonomic stabilization early in the Middle Triassic. Ammonoids and conodonts, by contrast, exhibit more rapid diversification in the Early Triassic followed by diversity decrease into the Middle Triassic. Carbon isotope data from Payne et al. (2004), brachiopod data from Chen et al. (2005), ammonoid data from Brayard et al. (2009), conodonts from Orchard (2007). Abbreviations and conodont zones as in Figure 3.

TABLE 3. Correlation (Spearman's *r*) between size and age in Griesbachian through Pelsonian genera, demonstrating that most genera exhibit a tendency toward size increase. The binomial probability of observing 11 of 13 genera exhibiting correlation in the same direction by chance is 0.02, suggesting that this pattern reflects a widespread tendency toward size increase within genera.

Genus	*r*	*p*-value	*n*
Diplotremina	0.217	0.58	9
Earlandia	0.100	0.80	9
Endoteba	−0.260	0.28	19
Endotebanella	0.119	0.59	23
Endotriadella	0.212	0.24	32
Hoyenella	0.386	0.003	59
Meandrospira	0.147	0.35	43
Pilammina	0.418	0.16	13
Pilamminella	0.750	0.02	9
Planiinvoluta	−0.371	0.47	6
Rectocornuspira	0.021	0.91	34
Reophax	0.333	0.38	9
Trochammina	0.024	0.96	8

TABLE 4. Correlation (Spearman's *r*) between size and age in Griesbachian through Pelsonian species. The binomial probability of observing eight of nine species exhibiting correlation in the same direction by chance is 0.04, suggesting that this pattern reflects a widespread tendency toward size increase within species.

Species	*r*	*p*-value	*n*
Endoteba bithynica	0.236	0.51	10
Endotriadella wirzi	0.067	0.74	26
Hoyenella ex gr. *sinensis*	0.323	0.02	51
Meandrospira dinarica	0.137	0.52	24
Meandrospira pusilla	−0.049	0.88	12
Pilammina densa	0.378	0.23	12
Pilamminella grandis	0.600	0.09	9
Rectocornuspira grandis	0.033	0.88	22
Rectocornuspira kalhori	0.051	0.81	24

through Aegean-Bithynian, demonstrating the progressive appearance of larger and larger taxa (Spearman *r* = 0.48, *p* = 0.006). Size increase was also widespread within species and genera. During the Griesbachian through Pelsonian, 11 of 13 genera and eight of nine species observed at six or more stratigraphic horizons exhibit positive correlation between size and stratigraphic position when tested using Spearman rank-order correlation coefficients (Tables 3, 4). Although the individual associations are not statistically significant for most species and genera, the overwhelming tendency toward size increase is not expected by chance (two-tailed binomial test: genera *p* = 0.02; species *p* = 0.04). These taxa represent a large fraction of occurrences of taxa within stratigraphic horizons (54% of genus occurrences, 38% of species occurrences) even though they constitute only a small fraction of the total taxonomic diversity (13/54 genera and 9/112 species), suggesting that their evolutionary dynamics may characterize the system as a whole.

Comparison to Carbon Cycle Dynamics.—The end-Permian mass extinction coincides with the first in a series of large carbon isotope excursions. These later isotope excursions may coincide with extinction and taxonomic turnover events in ammonoids and conodonts, and perhaps in the terrestrial flora as well (Galfetti et al. 2007b; Orchard 2007; Stanley 2009). In Figure 8 we present the δ^{13}C data of Payne et al. (2004) plotted against our recovery metrics. The foraminifers analyzed in this study derive from the same samples used to construct the δ^{13}C curve. The δ^{13}C data have been rescaled to geological time on the basis of radiometric constraints published subsequent to the δ^{13}C data (Mundil et al. 2004; Ovtcharova et al. 2005; Lehrmann et al. 2006; Galfetti et al. 2007a). The rescaled δ^{13}C data show a decrease in the rate of excursions through Early Triassic time that was not apparent when they were originally published with the more limited geochronological constraints. The gradual increases in diversity, evenness, and size among foraminifers on the GBG at the substage scale coincide with a gradual decrease in the rate of change in carbon isotopes.

Summary.—Taken as a whole, diversity, evenness, and size data suggest recovery of foraminifers on the GBG occurred steadily from the beginning of the Early Triassic through the early part of the Middle Triassic before stable Middle Triassic values of diversity, evenness, and size were achieved. The only evidence for decoupling between taxonomic and ecological recovery comes from a decrease in mean and maximum size between the Griesbachian and Dienerian, when sampling-standardized diversity and evenness were already increasing. All three metrics increased during the second half of the Early Triassic and achieved stable Middle Triassic values during Anisian time.

Increases in diversity and size do not merely reflect the sequential stacking of progressively more diverse habitats within stratigraphic sections; rather they occur within and among stratigraphic sections despite the clear overprint of a spatial diversity gradient. However, these differences in diversity between environments during Early and Middle Triassic time highlight the potential for isolated stratigraphic sections to exhibit patterns that either reduce or exaggerate the degree of regional recovery. As Payne et al. (2006a) found for trends in fossil abundance on the GBG, examination of the platform interior alone tends to reduce the apparent degree of recovery whereas examination of the basin margin alone tends to magnify the amount of biotic change occurring within Early Triassic time.

Discussion

Implications for Controls on Local Recovery Patterns.—The spatial gradient of decreasing diversity and abundance of foraminifers from shallow to deep water during the Griesbachian and Dienerian on the GBG is similar to that observed by Beatty et al. (2008) in trace fossil assemblages in onshore versus offshore settings in the Griesbachian and Dienerian of northwest Canada and is consistent with Twitchett et al.'s (2004) report of a diverse Griesbachian assemblage from a shallow-marine setting in Oman. On the GBG, oxygen depletion may have been an important limitation in slope environments during the Early Triassic and even, to a lesser extent, during the Late Permian (Payne et al. 2006a; Song et al. 2009). In contrast, restricted water circulation on the platform top behind a reef rim likely explains the lower diversity of platform interior environments in Middle Triassic time (Lehrmann et al. 1998; Payne et al. 2006b). These findings highlight the fact that recovery trends from isolated stratigraphic sections must be interpreted with caution because stacking of facies within stratigraphic sections can make it difficult to distinguish the effects of spatial gradients in diversity from global or regional secular trends.

Implications for Global Controls on Recovery.—The extinction and recovery pattern in foraminifers bears similarity to that of many benthic invertebrate clades in terms of diversity, abundance, and size patterns, suggesting it may be representative of the recovery of benthic ecosystems over larger spatial scales.

Global diversity increase in brachiopods (Chen et al. 2005) began in Smithian time but accelerated during the Anisian (Fig. 8), similar to the pattern observed in ostracods (Crasquin-Soleau et al. 2007) and foraminifers (Groves and Altiner 2005). Unlike conodonts and ammonoids, these benthic clades do not exhibit an Early Triassic diversity maximum. However, the lack of sampling-standardization in these studies prevents any explicit differentiation of sampling or preservation effects versus true diversity change.

Size reduction occurred between the Changhsingian and Griesbachian in numerous benthic clades, including gastropods (Fraiser and Bottjer 2004; Payne 2005), brachiopods (He et al. 2007; Twitchett 2007), and bivalves (Twitchett 2007). The pattern and timing of subsequent size increase in marine animals is less well known. Global and assemblage-level size data indicate that sizes had largely returned to pre-extinction distributions by Anisian time in gastropods (Fraiser and Bottjer 2004; Payne 2005; Twitchett 2007) and bivalves (Twitchett 2007). Some increase in gastropod mean and maximum size occurred during the Early Triassic (Payne 2005; Brayard et al. 2010), but most size increase occurred during the Anisian (Payne 2005). Such similarities between foraminifers and benthic invertebrates are not necessarily surprising, considering that benthic foraminifers live in the same habitats and exhibit many of the same trophic strategies as benthic invertebrates (Sen Gupta 2002).

Early Triassic dominance by species that are rare or absent during Middle Triassic time provides another parallel between the foraminiferan and benthic marine invertebrate fossil records. Lingulid brachiopods and small bivalve and gastropod mollusks commonly occur in high-abundance, low-diversity assemblages in Lower Triassic strata (Schubert and Bottjer 1995; Rodland and

Bottjer 2001) similar to those observed for *Rectocornuspira* and *Hoyenella* on the Great Bank of Guizhou. Similar communities are rare or absent from Middle Triassic normal-marine deposits (Fraiser and Bottjer 2005). Community-level recovery was not merely a process of addition to the associations established in the immediate aftermath of the end-Permian disturbance. Rather, substantial ecological reorganization and/or environmental change occurred that ultimately reduced or eliminated ecological opportunities for those taxa that thrived early in the aftermath of the mass extinction.

There is little indication of a lag interval during the recovery of foraminifers on the GBG. Size is the only recovery metric that does not show steady increase from the Griesbachian onward (Fig. 8). Despite the lack of a clearly defined lag interval, however, the recovery pattern is not easy to reconcile with simple models of unconstrained diversification. First, the rate of increase in sampling-standardized diversity and evenness is linear to convex, whereas nearly all models of uninhibited diversification predict an initially concave recovery trajectory (Fig. 1). Second, ecological modeling of taxonomic diversification by Solé et al. (2002) predicts recovery to occur most rapidly among primary producers and to subsequently propagate up the food chain to primary consumers and, finally, secondary consumers. In contrast, the Triassic fossil record reveals the most rapid diversification among higher taxa likely dominated by secondary consumers (ammonoids and conodonts) and more gradual diversification among taxa dominated by primary consumers (foraminifers, gastropods, bivalves, brachiopods, ostracods). The recovery rate of foraminifers was slower than that of ammonoids and conodonts, even though it appears more rapid than previously appreciated (Fig. 8).

Of course, simple models are not intended to capture all relevant processes; rather, they are intended as a point of comparison. Departures from model predictions can also yield insight, often by highlighting key factors and processes missing from the model. The most obvious missing factor in this case is the extent to which benthic and pelagic ecosystems are coupled. It is possible that both ecosystems were recovering along trajectories uninhibited by environmental conditions, but that the processes occurred more quickly in the pelagic realm. However, chemical stratification of the Early Triassic water column (Wignall and Twitchett 2002; e.g., Grice et al. 2005; Meyer et al. 2008, 2011) may also account for the more rapid recovery of pelagic organisms. Most ammonoids and conodonts likely inhabited the shallow, well-mixed, oxygenated part of the marine water column and had the ability to migrate if they encountered harmful water masses. Moreover, ammonoids may have been physiologically well-adapted to low-oxygen conditions (Marshall and Jacobs 2009). This latter view is further supported by the fact that ammonoids and conodonts did not simply diversify more rapidly than benthic clades. They also reached diversity maxima during Early Triassic time and declined in diversity across the Early–Middle Triassic transition, suggesting Early Triassic oceans were in fact more favorable than Middle Triassic oceans for these groups. This pattern stands in sharp contrast to the permanent and stable increase in both taxonomic and ecological recovery metrics observed in foraminifers and other benthic groups from the Early to Middle Triassic.

Conclusions

We observe a steady and gradual increase in the diversity, evenness, and size of foraminifers on the Great Bank of Guizhou during the Early Triassic, with stable values achieved early in Middle Triassic time. This pattern is robust to sampling standardization within and among local habitats spanning a gradient from shallow-water platform interior to deeper-water basin margin environments, indicating that it represents a platform-wide recovery trajectory. Similarities in pattern and timing of recovery of foraminifers on the GBG and their recovery globally indicate that the local pattern is representative of regional to global processes. Our findings suggest that recovery of at least some benthic clades proceeded steadily through Early Triassic time and that an Early Triassic recovery lag, if it exists, characterizes only the recovery of

certain taxa or environments. The trajectory of recovery in foraminifers is similar to that of many benthic marine invertebrates, but more gradual than that of well-studied pelagic taxa such as ammonoids and conodonts. These findings suggest a decoupling of recovery processes between benthic and pelagic environments. However, it remains unclear whether the contrasting recovery trajectories result from differences in environmental controls or intrinsic processes of diversification. The gradual decrease in the rate of carbon isotope excursions through the Early Triassic is suggestive of gradual environmental amelioration, although the strong influence of benthic organisms on the global sulfur and carbon cycles (Canfield and Farquhar 2009) leaves open the possibility that gradual stabilization of biogeochemical cycling was a consequence of biotic recovery rather than a cause. As details are added to our picture of recovery from the end-Permian extinction, it increasingly appears that insights into recovery mechanisms will come not from determining whether or not recovery was delayed but, rather, from understanding why recovery trajectories differ among habitats and higher taxa.

Acknowledgments

Literature Cited

Adachi, N., Y. Ezaki, and J. B. Liu. 2004. The fabrics and origins of peloids immediately after the end-Permian extinction, Guizhou Province, south China. Sedimentary Geology 164:161–178.

Apthorpe, M. 2003. Early to lowermost Middle Triassic Foraminifera from the Locker Shale of Hampton-1 well, Western Australia. Journal of Micropalaeontology 22:1–27.

Baud, A., S. Richoz, and S. B. Pruss. 2007. Lower Triassic anachronistic carbonate facies in space and time. Global and Planetary Change 55:81–89.

Beatty, T. W., J.-P. Zonneveld, and C. M. Henderson. 2008. Anomalously diverse Early Triassic ichnofossil assemblages in northwest Pangea: a case for a shallow-marine habitable zone. Geology 36:771–774.

Beauchamp, B., and A. Baud. 2002. Growth and demise of Permian biogenic chert along northwest Pangea: evidence for end-Permian collapse of thermohaline circulation. Palaeogeography, Palaeoclimatology, Palaeoecology 184:37–63.

Brayard, A., G. Escarguel, H. Bucher, C. Monnet, T. Bruhwiler, N. Goudemand, T. Galfetti, and J. Guex. 2009. Good genes and good luck: ammonoid diversity and the end-Permian mass extinction. Science 325:1118–1121.

Brayard, A., A. Nutzel, D. A. Stephen, K. G. Bylund, J. Jenks, and H. Bucher. 2010. Gastropod evidence against the Early Triassic Lilliput effect. Geology 38:147–150.

Canfield, D. E., and J. Farquhar. 2009. Animal evolution, bioturbation, and the sulfate concentration of the oceans. Proceedings of the National Academy of Sciences USA 106:8123–8127.

Chen, Z.-Q., K. Kaiho, and A. D. George. 2005. Early Triassic recovery of the brachiopod faunas from the end-Permian mass extinction: a global review. Palaeogeography, Palaeoclimatology, Palaeoecology 224:270–290.

Crasquin-Soleau, S., T. Galfetti, H. Bucher, S. Kershaw, and Q. Feng. 2007. Ostracod recovery in the aftermath of the Permian-Triassic crisis: Palaeozoic-Mesozoic turnover. Hydrobiologia 585:13–27.

Erwin, D. H. 1993. The great Paleozoic crisis: life and death in the Permian. Columbia University Press, New York.

———. 2001. Lessons from the past: biotic recoveries from mass extinctions. Proceedings of the National Academy of Sciences USA 98:5399–5403.

———. 2007. Increasing returns, ecological feedback and the Early Triassic recovery. Palaeoworld 16:9–15.

Ezaki, Y., J. Liu, T. Nagano, and N. Adachi. 2008. Geobiological aspects of the earliest Triassic microbialites along the southern periphery of the tropical Yangtze Platform: initiation and cessation of a microbial regime. Palaios 23:356–369.

Flügel, E. 1994. Pangean shelf carbonates: controls and paleoclimatic significance of Permian and Triassic reefs. In G. D. Klein, ed. Pangea: paleoclimate, tectonics, and sedimentation during accretion, zenith, and breakup of a supercontinent. Geological Society of America Special Paper 288:247–266.

———. 2002. Triassic reef patterns. In W. Kiessling, E. Flügel, and J. Golonka, eds. Phanerozoic reef patterns. SEPM Special Publication 72:291–464. Society for Sedimentary Geology, Tulsa, Okla.

Fraiser, M. L., and D. J. Bottjer. 2004. The non-actualistic Early Triassic gastropod fauna: a case study of the Lower Triassic Sinbad Limestone member. Palaios 19:259–275.

———. 2005. Restructuring in benthic level-bottom shallow marine communities due to prolonged environmental stress following the end-Permian mass extinction. Comptes Rendus Palevol 4:515–523.

———. 2007. Elevated atmospheric CO_2 and the delayed biotic recovery from the end-Permian extinction. Palaeogeography, Palaeoclimatology, Palaeoecology 252:164–175.

Galfetti, T., H. Bucher, M. Ovtcharova, U. Schaltegger, A. Brayard, T. Brühwiler, N. Goudemand, H. Weissert, P. A. Hochuli, F. Cordey, and G. Kuang. 2007a. Timing of the Early Triassic carbon cycle perturbations inferred from new U-Pb ages and ammonoid biochronozones. Earth and Planetary Science Letters 258:593–604.

Galfetti, T., P. A. Hochuli, A. Brayard, H. Bucher, H. Weissert, and J. O. Vigran. 2007b. Smithian-Spathian boundary event:

evidence for global climatic change in the wake of the end-Permian biotic crisis. Geology 35:291–294.

Grice, K., C. Q. Cao, G. D. Love, M. E. Bottcher, R. J. Twitchett, E. Grosjean, R. E. Summons, S. C. Turgeon, W. Dunning, and Y. G. Jin. 2005. Photic zone euxinia during the Permian-Triassic superanoxic event. Science 307:706–709.

Groves, J. R., and D. Altiner. 2005. Survival and recovery of calcareous foraminifera pursuant to the end-Permian mass extinction. Comptes Rendus Palevol 4:419–432.

Groves, J. R., D. Altiner, and R. Rettori. 2005. Extinction, survival, and recovery of lagenide foraminifers in the Permian-Triassic boundary interval, central Taurides, Turkey. Journal of Paleontology Memoir 62:1–38.

Groves, J. R., R. Rettori, J. L. Payne, M. D. Boyce, and D. Altiner. 2007. End-Permian mass extinction of lagenide foraminifers in the southern Alps (northern Italy). Journal of Paleontology 81:415–434.

Hallam, A. 1991. Why was there a delayed radiation after the end-Paleozoic extinctions? Historical Biology 5:257–262.

Hammer, Ø., D. A. T. Harper, and P. D. Ryan. 2001. PAST: paleontological statistics software package for education and data analysis. Palaeontologia Electronica 4:1–9.

Hauser, M., R. Martini, S. Burns, P. Dumitrica, L. Krystyn, A. Matter, T. Peters, and L. Zaninetti. 2001. Triassic stratigraphic evolution of the Arabian–Greater India embayment of the southern Tethys margin. Eclogae Geologicae Helvetiae 94:29–62.

He, W., G. R. Shi, Q. Feng, M. J. Campi, S. Gu, J. Bu, Y. Peng, and Y. Meng. 2007. Brachiopod miniaturization and its possible causes during the Permian-Triassic crisis in deep water environments, South China. Palaeogeography, Palaeoclimatology, Palaeoecology 252:145–163.

Hurlbert, S. H. 1971. The nonconcept of species diversity: a critique and alternative parameters. Ecology 52:577–586.

Jacobsen, N. D., R. J. Twitchett, and L. Krystyn. 2010. Palaeoecological methods for assessing marine ecosystem recovery following the Late Permian mass extinction event. Palaeogeography, Palaeoclimatology, Palaeoecology in press.

Knoll, A. H., R. K. Bambach, J. L. Payne, S. Pruss, and W. W. Fischer. 2007. Paleophysiology and end-Permian mass extinction. Earth and Planetary Science Letters 256:295–313.

Kobayashi, F. 1997. Upper Permian foraminifers from the Iwai-Kanyo area, West Tokyo, Japan. Journal of Foraminiferal Research 27:186–195.

———. 2004. Late Permian foraminifers from the limestone block in the southern Chichibu Terrane of West Shikoku, SW Japan. Journal of Paleontology 78:62–70.

———. 2005. Permian foraminifers from the Itsukaichi-Ome area, west of Tokyo, Japan. Journal of Paleontology 79:413–432.

Kobayashi, F., R. Martini, and L. Zaninetti. 2005. Anisian foraminifers from allochthonous limestones of the Tanoura formation (Kurosegawa Terrane, West Kyushu, Japan). Geobios 38:751–763.

Krull, E. S., D. J. Lehrmann, D. Druke, B. Kessel, Y. Y. Yu, and R. X. Li. 2004. Stable carbon isotope stratigraphy across the Permian-Triassic boundary in shallow marine carbonate platforms, Nanpanjiang Basin, south China. Palaeogeography, Palaeoclimatology, Palaeoecology 204:297–315.

Lehrmann, D. J. 1999. Early Triassic calcimicrobial mounds and biostromes of the Nanpanjiang basin, south China. Geology 27:359–362.

Lehrmann, D. J., J. Y. Wei, and P. Enos. 1998. Controls on facies architecture of a large Triassic carbonate platform: the Great Bank of Guizhou, Nanpanjiang Basin, south China. Journal of Sedimentary Research 68:311–326.

Lehrmann, D. J., Y. Wan, J. Y. Wei, Y. Y. Yu, and J. F. Xiao. 2001. Lower Triassic peritidal cyclic limestone: an example of anachronistic carbonate facies from the Great Bank of Guizhou,

Nanpanjiang Basin, Guizhou Province, South China. Palaeogeography, Palaeoclimatology, Palaeoecology 173:103–123.

Lehrmann, D. J., J. L. Payne, S. V. Felix, P. M. Dillett, H. Wang, Y. Y. Yu, and J. Y. Wei. 2003. Permian-Triassic boundary sections from shallow-marine carbonate platforms of the Nanpanjiang Basin, south China: implications for oceanic conditions associated with the end-Permian extinction and its aftermath. Palaios 18:138–152.

Lehrmann, D. J., J. Ramezani, M. W. Martin, S. A. Bowring, P. Montgomery, P. Enos, J. L. Payne, M. J. Orchard, H.-M. Wang, and J. Wei. 2006. Timing of biotic recovery from the end-Permian extinction: biostratigraphic and geochronologic constraints from south China. Geology 34:1053–1056.

Lehrmann, D. J., D. Pei, P. Enos, M. Minzoni, B. Ellwood, M. J. Orchard, J. Zhang, J. Wei, P. Dillett, J. Koenig, K. Steffen, D. Druke, J. Druke, B. Kessel, and T. Newkirk. 2007. Impact of differential tectonic subsidence on isolated carbonate-platform evolution: Triassic of the Nanpanjiang Basin, south China. American Association of Petroleum Geologists Bulletin 91:287–320.

Leven, E. J., and A. I. Okay. 1996. Foraminifera from the exotic Permo-Carboniferous limestone blocks in the Karakaya Complex, Northwestern Turkey. Rivista Italiana di Paleontologia e Stratigrafia 102:139–174.

Marshall, C. R., and D. K. Jacobs. 2009. Flourishing after the end-Permian mass extinction. Science 325:1079–1080.

Meyer, K. M., L. R. Kump, and A. Ridgwell. 2008. Biogeochemical controls on photic-zone euxinia during the end-Permian mass extinction. Geology 36:747–750.

Meyer, K. M., M. Yu, A. B. Jost, B. M. Kelley, and J. L. Payne. 2011. $\delta^{13}C$ evidence that high primary productivity delayed the end-Permian mass extinction. Earth and Planetary Science Letters 302:378–384.

Mundil, R., P. Brack, M. Meier, H. Rieber, and F. Oberli. 1996. High resolution U-Pb dating of Middle Triassic volcaniclastics: Time-scale calibration and verification of tuning parameters for carbonate sedimentation. Earth and Planetary Science Letters 141:137–151.

Mundil, R., K. R. Ludwig, I. Metcalfe, and P. R. Renne. 2004. Age and timing of the Permian mass extinctions: U/Pb dating of closed-system zircons. Science 305:1760–1763.

Novack-Gottshall, P. M. 2008. Using simple body size metrics to estimate fossil body volume: empirical validation using diverse Paleozoic invertebrates. Palaios 23:163–173.

Orchard, M. J. 2007. Conodont diversity and evolution through the latest Permian and Early Triassic upheavals. Palaeogeography, Palaeoclimatology, Palaeoecology 252:93–117.

Ovtcharova, M., H. Bucher, and U. Schaltegger. 2005. Calibration of the early Triassic biotic recovery: New U/Pb zircon ages from South China. Geochimica et Cosmochimica Acta 69:A324–A324.

Ovtcharova, M., H. Bucher, U. Schaltegger, T. Galfetti, A. Brayard, and J. Guex. 2006. New Early to Middle Triassic U-Pb ages from South China: calibration with ammonoid biochronozones and implications for the timing of the Triassic biotic recovery. Earth and Planetary Science Letters 243:463–475.

Payne, J. L. 2005. Evolutionary dynamics of gastropod size across the end-Permian extinction and through the Triassic recovery interval. Paleobiology 31:269–290.

Payne, J. L., D. J. Lehrmann, J. Wei, M. J. Orchard, D. P. Schrag, and A. H. Knoll. 2004. Large perturbations of the carbon cycle during recovery from the end-Permian extinction. Science 305:506–509.

Payne, J. L., D. J. Lehrmann, J. Wei, and A. H. Knoll. 2006a. The pattern and timing of biotic recovery from the end-Permian extinction on the Great Bank of Guizhou, Guizhou Province, China. Palaios 21:63–85.

Payne, J. L., D. J. Lehrmann, S. Christensen, J. Wei, and A. H. Knoll. 2006b. Environmental and biological controls on the initiation and growth of a Middle Triassic (Anisian) reef complex on the Great Bank of Guizhou, Guizhou Province, China. Palaios 21:325–343.

Payne, J. L., D. J. Lehrmann, D. Follett, M. Seibel, L. R. Kump, A. Riccardi, D. Altiner, H. Sano, and J. Wei. 2007. Erosional truncation of uppermost Permian shallow-marine carbonates and implications for Permian-Triassic boundary events. Geological Society of America Bulletin 119:771–784.

Pronina-Nestell, G. P., and M. K. Nestell. 2001. Late Changhsingian foraminifers of the northwestern Caucasus. Micropaleontology 47:205–234.

Pruss, S. B., and D. J. Bottjer. 2004. Late Early Triassic microbial reefs of the western United States: a description and model for their deposition in the aftermath of the end-Permian mass extinction. Palaeogeography, Palaeoclimatology, Palaeoecology 211:127–137.

Pruss, S. B., F. A. Corsetti, and D. J. Bottjer. 2005a. Environmental trends of Early Triassic biofabrics: implications for understanding the aftermath of the end-Permian mass extinction. Pp. 313–332 in J. D. Morrow, D. J. Over, and P. B. Wignall, eds. Understanding Late Devonian and Permian-Triassic biotic and climatic events: toward an integrated approach. Elsevier, Amsterdam.

———. 2005b. The unusual sedimentary rock record of the Early Triassic: a case study from the southwestern United States. Palaeogeography, Palaeoclimatology, Palaeoecology 222:33–52.

Pruss, S. B., D. J. Bottjer, F. A. Corsetti, and A. Baud. 2006. A global marine sedimentary response to the end-Permian mass extinction: examples from southern Turkey and the western United States. Earth-Science Reviews 78:193–206.

Retallack, G. J. 1999. Postapocalyptic greenhouse paleoclimate revealed by earliest Triassic paleosols in the Sydney Basin, Australia. Geological Society of America Bulletin 111:52–70.

Retallack, G. J., J. J. Veevers, and R. Morante. 1996. Global coal gap between Permian-Triassic extinction and Middle Triassic recovery of peat-forming plants. Geological Society of America Bulletin 108:195–207.

Rettori, R. 1995. Foraminiferi del Trias inferiore e medio della Tetide: Revisione tassonomica, stratigrafia ed interpretazione filogenetica. Publications du départment de géologie et paléontologie: Université de Genève 18:1–149.

Rodland, D. L., and D. J. Bottjer. 2001. Biotic recovery from the end-Permian mass extinction: Behavior of the inarticulate brachiopod Lingula as a disaster taxon. Palaios 16:95–101.

Salaj, J., K. Borza, and O. Samuel. 1983. Triassic foraminifers of the west Carpathians. Geologický ústav Dionýza Štúra, Bratislava.

Schell, W. W., and D. L. Clark. 1960. Lower Triassic foraminifera from Nevada. Micropaleontology 6:291–296.

Schroeder, M. L. 1968. Lower Triassic foraminifera from the Thaynes Formation in southeastern Idaho and western Wyoming. Micropaleontology 14:73–82.

Schubert, J. K., and D. J. Bottjer. 1995. Aftermath of the Permian-Triassic mass extinction event—Paleoecology of Lower Triassic carbonates in the western USA. Palaeogeography, Palaeoclimatology, Palaeoecology 116:1–39.

Sen Gupta, B. K. 2002. Modern Foraminifera. Kluwer, Boston.

Solé, R. V., J. M. Montoya, and D. H. Erwin. 2002. Recovery after mass extinction: evolutionary assembly in large-scale biosphere dynamics. Philosophical Transactions of the Royal Society of London Series B-Biological Sciences 357:697–707.

Song, H.-J., J.-N. Tong, K.-X. Zhang, Q.-X. Wang, and Z. Q. Chen. 2007. Foraminiferal survivors from the Permian-Triassic mass extinction in the Meishan section, South China. Palaeoworld 16:105–119.

Song, H., J. Tong, Z. Q. Chen, H. A. O. Yang, and Y. Wang. 2009. End-Permian mass extinction of foraminifers in the Nanpanjiang Basin, south China. Journal of Paleontology 83:718–738.

Stanley, S. M. 2009. Evidence from ammonoids and conodonts for multiple Early Triassic mass extinctions. Proceedings of the National Academy of Sciences USA 106:15264–15267.

Tong, J., J. Zuo, and Z. Q. Chen. 2007. Early Triassic carbon isotope excursions from south China: proxies for devastation and restoration of marine ecosystems following the end-Permian mass extinction. Geological Journal 42:371–389.

Twitchett, R. J. 1999. Palaeoenvironments and faunal recovery after the end-Permian mass extinction. Palaeogeography, Palaeoclimatology, Palaeoecology 154:27–37.

———. 2001. Incompleteness of the Permian-Triassic fossil record: a consequence of productivity decline? Geological Journal 36:341–353.

———. 2007. The Lilliput effect in the aftermath of the end-Permian extinction event. Palaeogeography, Palaeoclimatology, Palaeoecology 252:132–144.

Twitchett, R. J., and P. B. Wignall. 1996. Trace fossils and the aftermath of the Permo-Triassic mass extinction: evidence from northern Italy. Palaeogeography, Palaeoclimatology, Palaeoecology 124:137–151.

Twitchett, R. J., L. Krystyn, A. Baud, J. R. Wheeley, and S. Richoz. 2004. Rapid marine recovery after the end-Permian mass-extinction event in the absence of marine anoxia. Geology 32:805–808.

Unal, E., D. Altiner, I. O. Yilmaz, and S. Ozkan-Altiner. 2003. Cyclic sedimentation across the Permian-Triassic boundary (Central Taurides, Turkey). Rivista Italiana di Paleontologia e Stratigrafia 109:359–376.

Vuks, V. J. 2007. Olenekian (Early Triassic) foraminifers of the Gorny Mangyshlak, eastern Precaucasus and western Caucasus. Palaeogeography, Palaeoclimatology, Palaeoecology 252:82–92.

Wignall, P. B., and R. J. Twitchett. 2002. Extent, duration, and nature of the Permian-Triassic superanoxic event. In C. Koeberl and K. G. MacLeod, eds. Catastrophic events and mass extinctions; impacts and beyond. Geological Society of America Special Publication 356:395–413.

Yang, W., and D. J. Lehrmann. 2003. Milankovitch climatic signals in Lower Triassic (Olenekian) peritidal carbonate successions, Nanpanjiang Basin, South China. Palaeogeography, Palaeoclimatology, Palaeoecology 201:283–306.

Zaninetti, L. 1976. Les foraminifères du Trias—essai de synthèse et corrélation entre les domaines mésogéens européen et asiatique. Rivista Italiana di Paleontologia 82:1–258.